JOM 23557

Electrospray mass spectrometry of inert and labile metal alkyl compounds: a study of methyl and dimethyl derivatives of gold(III), indium(III) and thallium(III)

Allan J. Canty

Chemistry Department, University of Tasmania, Hobart, Tasmania 7001 (Australia)

Ray Colton and Ian M. Thomas

Chemistry Department, La Trobe University, Bundoora, Vic. 3083 (Australia)

(Received December 21, 1992)

Abstract

Electrospray mass spectra have been obtained from methanol solution for a number of cationic methyl and dimethyl derivatives of gold(III), indium(III) and thallium(III), the other ligands being usually polydentate nitrogen bases. The gold compounds were all non-labile dimethyl derivatives and they invariably gave the principal ion in the ES mass spectrum, but loss of both methyl groups could be achieved by collisional activation within the ion source, especially at higher ion source energies. Collisionally activated decomposition (CAD) mass spectra were also investigated by tandem mass spectrometry using argon, and the mode of further fragmentation depended upon the nature of the polydentate nitrogen ligand. Some of the indium(III) complexes also gave the principal ion, but for those cations containing a coordinated water molecule in the solid state the ion of highest m/z observed was the daughter ion corresponding to loss of water from the principal ion. The ES mass spectra of dimeric species of the type $[(MeIn)_2L_2(NO_3)(H_2O)]^+$ (L is a polydentate bridging alkoxide ligand), which are known to be labile in solution, give $[(MeIn)_2L_2]^{2+}$ as the base peak, but they do also show ions corresponding to $[(MeIn)_2L_2(NO_3)]^+$ or $[(MeIn)_2L_2(OAc)]^+$, the acetate originating from the mobile phase used in the spectrometer. In the solid state, the thallium complexes all contain either coordinated water ligands or bridging nitrato groups and some of them are not ionic in the solid state. The cationic thallium compounds do not show the principal ions in their ES mass spectra, but rather the daughter ions expected by loss of water. The neutral solid state polymeric species gives ions in their ES mass spectra corresponding to loss of the nitrato groups in solution, but the weakly coordinated nitrogen bases are retained in the ES mass spectra.

1. Introduction

The main obstacle to the study of the mass spectra of inorganic and organometallic compounds has been the process of generating ions in the gas phase. The original ionisation technique of electron impact (EI) frequently led to extensive fragmentation, although the molecular ion was sometimes observed as a low intensity peak [1]. Consequently, considerable efforts have been made to devise softer ionisation techniques and fast atom bombardment mass spectrometry (FAB/MS) has been one of the more successful. In the study of neutral species it often generates the molecular ion [2] and in the case of ionic compounds there have been numerous cases in which the principal ion has been observed [3–6].

The new technique of electrospray ionisation, largely developed by Fenn and his co-workers [7–9], provides a method of transferring pre-existing ions from solution to the gas phase. The transfer is very soft and causes minimal fragmentation. Although electrospray mass spectrometry (ESMS) is now a well established technique in the structural analysis of large biomolecules such as proteins [10,11], and the increase in publications utilising the technique is now almost exponential [12], reports of its application to inorganic and organometallic systems are still few in number.

We have recently been investigating the use of ESMS on a range of charged inorganic and organometallic

Correspondence to: Dr. R. Colton.

0022-328X/93/$6.00

compounds [13–16]. A feature of these studies is that the principal ions were always observed, often as the only significant peak in the mass spectrum, emphasising the soft nature of the process generating the gas phase ions. In the case of very labile species, such as $[Cu(PPh_3)_3]^+$ [16], daughter ions formed by collisional activation within the electrospray ion source were also observed.

The term principal ion is used [17] to indicate that the ion observed in the gas phase is the same as that pre-existing in the solution, in contrast to a molecular ion which is formed from a neutral species within the mass spectrometer.

In this paper we apply the ESMS technique to a series of methyl and dimethyl derivatives of gold(III), indium(III) and thallium(III) in which the other ligands are usually polydentate nitrogen bases. These cationic complexes were chosen for initial investigation because structural studies have been reported for most of them [18–22], and the structures exhibit a gradation from strong metal–nitrogen bonding in the gold(III) complexes [Au–N: 2.024(9)–2.041(12) Å] to very weak bonding in the thallium(III) complexes [Tl–N: 2.61(3)–2.666(9) Å].

2. Results and discussion

Throughout this paper peaks in the mass spectra will be identified by the most intense m/z value in the isotopic mass distribution. In all cases the experimental and calculated isotopic mass distributions were in good agreement.

2.1. Gold(III) compounds

Several square planar dimethylgold(III) complexes $[Me_2Au(L)]NO_3$ were examined. The ligands are illustrated in Scheme 1; they act as bidentates with the uncoordinated phenyl or pyridine groups adopting orientations in the solid state above the square plane in the complexes of py_3CH, py_2PhCH and $pymim_2COH$ [18,20].

Figure 1a shows the positive ion ES mass spectrum of $[Me_2Au(py_3CH)]NO_3$ at an ion source energy (B1 voltage) of 40 V. The dominant peak is due to the principal ion $[Me_2Au(py_3CH)]^+$ (m/z 474), and the smaller peak at m/z 444 is caused by loss of Me_2 to give the daughter ion $[Au(py_3CH)]^+$. Figure 1(b) shows the ES mass spectrum at a slightly higher ion source energy (B1 = 60 V), and under these conditions the daughter ion is the base peak, showing that both methyl groups are readily lost from the gold cation in the gas phase. The almost total lack of other peaks is typical of the quality of spectra recorded for the compounds discussed in this paper. Figure 1(c) is a comparison of

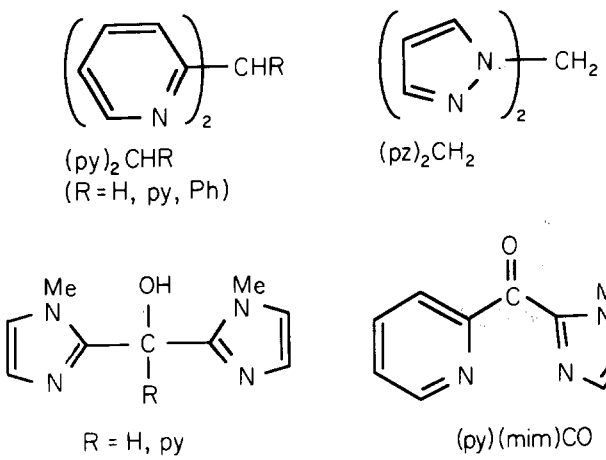

Scheme 1. Ligands present in $[Me_2Au(L)]^+$.

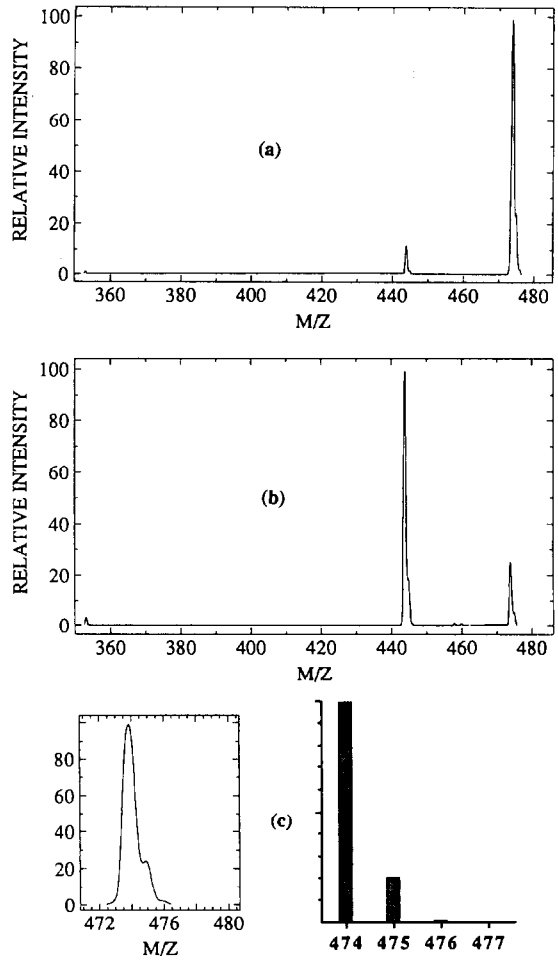

Fig. 1. Positive ion ES mass spectrum of $[Me_2Au(py_3CH)]NO_3$: (a) B1 voltage = 40 V; (b) B1 voltage = 60 V; (c) comparison of experimental and calculated isotopic mass distribution for m/z 474.

the experimental and calculated isotopic mass distribution for the principal ion. MS/MS experiments on the m/z 474 ion in the absence of any gas in the collision cell show that it is metastable, with about 10% of the ions losing both methyl groups on the timescale of this experiment (~ 100 μs). In the presence of argon in the collision cell, enhanced loss of both methyl ligands occurs and peaks due to $[L-H]^+$ (m/z 246) and $[L-H-py]^+$ (m/z 168) ($L = py_3CH$) are also observed in the collisional activated decomposition (CAD) mass spectrum. No ions containing gold, other than that at m/z 444, were observed in the CAD mass spectrum for this compound. Data for this and all other compounds are given in Table 1. In all cases the ions recorded in Table 1 for the ES mass spectra are those observed at low ion source energies. Any daughter ions listed in the ES mass spectra are always observed in the CAD mass spectra also, but they are not tabulated twice. The ESMS results for $[Me_2Au(py_2PhCH)]NO_3$ and $[Me_2Au(py_2CH_2)]NO_3$, which also contain pyridine based nitrogen ligands, are completely analogous to those of $[Me_2Au(py_3CH)]NO_3$, and all data are given in Table 1.

The ES mass spectra at low ion source energies of a series of dimethyl gold compounds compounds containing ligands based upon imidazoles, such as $[Me_2Au\{mim_2CH(OH)\}]NO_3$ and $[Me_2Au(pymimCO)]NO_3$, also give their principal ions together with the daughter ions resulting from loss of both methyl groups. However, the CAD mass spectra show a different pattern of fragmentation with the observation of the daughter ion $[Au(mimH)]^+$, containing gold and a portion of the imidazole ligand, in each case (Table 1). This indicates greater strength of the gold–nitrogen bond in the imidazole derivatives, compared with the pyridine compounds.

The compound $[Me_2Au(pymim_2COH)]NO_3$, in which the potentially tridentate ligand is acting as a bidentate with an uncoordinated pyridine group [20], also gives its principal ion (m/z 496) and the daughter resulting from the loss of both methyl groups. However, it also undergoes collisionally activated decomposition within the ion source resulting in the loss of (mim + H) to give the ion $[Me_2Au(pymimCO)]^+$ (m/z 414) discussed above, and its daughter ion $[Au(pymimCO)]^+$ (m/z 384).

The compound $Me_2Au(pz_3BH)$ is known [20] to undergo protonation quite readily, therefore although it is neutral and not amenable to ESMS it is in fact protonated by the mobile phase (H_2O/MeOH/1% HOAc) used in the spectrometer so that the cation $[Me_2Au\{(Hpz)pz_2BH\}]^+$ is observed. At low ion source energies the principal ion (m/z 441) is the base peak with the only other significant peak being at m/z 373 $[Me_2Au(pz_2BH)]^+$ but there is no peak at m/z 411 corresponding to loss of both methyl groups from the principal ion. At higher ion source energies the signal at m/z 373 becomes the base peak and another signal appears at m/z 343 due to $[Au(pz_2BH)]^+$.

2.2. *Indium(III) compounds*

The dimethylindium(III) complexes studied here have much weaker metal–nitrogen interactions than the dimethylgold(III) compounds. Complexes for which

TABLE 1. Electrospray mass spectrometric data for gold compounds

Compound	Ions in ES mass spectra (m/z) [a]	Ions in CAD mass spectra (m/z)
$[Me_2Au(py_3CH)]NO_3$	$[Me_2Au(py_3CH)]^+$ (474) $[Au(py_3CH)]^+$ (444)	$[py_3C]^+$ (246), $[py_2C]^+$ (168)
$[Me_2Au(py_2PhCH)]NO_3$	$[Me_2Au(py_2PhCH)]^+$ (473) $[Au(py_2PhCH)]^+$ (443)	$[py_2PhC]^+$ (245), $[pyPhC]^+$ (167)
$[Me_2Au(py_2CH_2)]NO_3$	$[Me_2Au(py_2CH_2)]^+$ (397) $[Au(py_2CH_2)]^+$ (367)	$[py_2CH]^+$ (169)
$[Me_2Au\{mim_2CH(OH)\}]NO_3$	$[Me_2Au\{mim_2CH(OH)\}]^+$ (419) $[Au(mimH)]^+$ (279) $[Au\{mim_2CH(OH)\}]^+$ (389)	
$[Me_2Au(pymimCO)]NO_3$	$[Me_2Au(pymimCO)]^+$ (414) $[Au(pymimCO)]^+$ (384)	$[Au(mimH)]^+$ (279)
$[Me_2Au(pymim_2COH)]NO_3$	$[Me_2Au(pymim_2COH)]^+$ (496) $[Au(pymim_2COH)]^+$ (466) $[Me_2Au(pymimCO)]^+$ (414) $[Au(pymimCO)]^+$ (384)	$[Au(mimH)]^+$ (279)
$[Me_2Au(pz_2CH_2)]NO_3$	$[Me_2Au(pz_2CH_2)]^+$ (375) $[Au(pz_2CH_2)]^+$ (345)	$[Au(pzCH)]^+$ (277) $[Au(pzH)]^+$ (265)
$[Me_2Au\{(Hpz)pz_2BH\}]^+$	$[Me_2Au\{(Hpz)pz_2BH\}]^+$ (441) $[Me_2Au(pz_2BH)]^+$ (373)	

[a] Ions observed at low ion source energies.

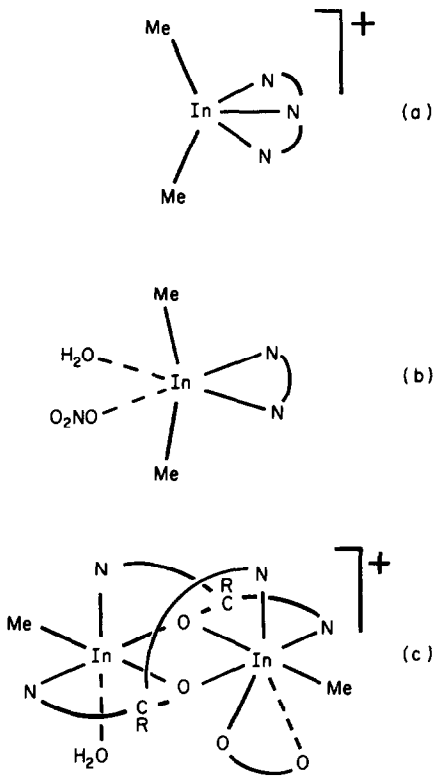

Scheme 2. Structures of indium complexes in the solid state: (a) $[Me_2In(Et_3terpy)]NO_3$: InC_2 132.8(3)°, In–N 2.310(5)–2.360(6) Å; (b) $Me_2In(py_2CH_2)(NO_3)(H_2O)$: InC_2 157.6(2)°, In–N 2.42(4)–2.439(4), In–ONO_2 2.632(4), In–OH_2 2.679(5) Å; (c) $[(MeIn)_2(L)_2(NO_3)(H_2O)]NO_3$: alkoxide dimer, drawn with idealised geometries, on comparison with the crystal structures of the $(py)_2PhCO^-$ and $(py)(mim)_2CO^-$ analogues.

structural studies have been reported are shown in Scheme 2, together with the robust binuclear MeIn(III) complexes.

The five coordinate complex $[Me_2In(Et_3terpy)]NO_3$ [21] nicely illustrates the different ESMS behaviour of indium complexes. At low ion source energies (B1 = 40 V) the principal ion $[Me_2In(Et_3terpy)]^+$ (m/z 462) is the dominant peak, the only other significant peak is due to $[Et_3terpyH]^+$ (m/z 318). Even at B1 = 80 V only a small peak is observed for the daughter ion formed by loss of the two methyl groups, but at B1 = 100 V there is significant formation of $[In(Et_3terpy)]^+$ (m/z 432) and also $[Me_2In]^+$ (m/z 145). As with the gold complexes, there is no indication of a daughter ion containing one methyl group. In the MS/MS with selected ions of m/z 462 in the absence of gas in the collision cell, there is no decomposition at all, showing the ion to be stable in the gas phase on the timescale of the experiment. In the presence of argon in the collision cell the ions $[In(Et_3terpy)]^+$ (m/z 432), $[Me_2In]^+$ (m/z 145) and In^+ (m/z 115) are also observed. The ion $[Et_3terpyH]^+$ (m/z 318) is not observed in the CAD mass spectrum which indicates that its appearance in the ES mass spectrum results from reactions in the ion source. Presumably some dissociation of the ligand is followed by protonation by the acetic acid present in the mobile phase. Electrospray mass spectrometric data for all the indium compounds studied are given in Table 2.

The compound $Me_2In(py_2CH_2)(H_2O)(NO_3)$ has a weakly bound nitrato ligand in the solid state, but the

TABLE 2. Electrospray mass spectrometric data for indium and thallium compounds

Compound	Ions in ES mass spectra (m/z) [a]
$[Me_2In(Et_3terpy)]NO_3$	$[Me_2In(Et_3terpy)]^+$ (462); $[Et_3terpyH]^+$ (318)
$[Me_2In(py_2CH_2)(H_2O)]NO_3$	$[Me_2In(py_2CH_2)]^+$ (315); $[Hpy_2CH_2]^+$(171)
$[(MeIn)_2L_2(NO_3)(H_2O)]NO_3$ ($L = py_3CO$)	$[(MeIn)_2L_2(OAc)]^+$ (843); $[In\{(py_3)CO\}_2]^+$ (639); $[(MeIn)_2L_2]^{2+}$ (392)
$[(MeIn)_2L_2(NO_3)(H_2O)]NO_3$ ($L = py_2PhCO$)	$[(MeIn)_2L_2(OAc)]^+$ (841); $[In\{(py_2Ph)CO\}_2]^+$ (637); $[(MeIn)_2L_2]^{2+}$ (391)
$[(MeIn)_2L_2(NO_3)(H_2O)]NO_3$ ($L = pymim_2CO$)	$[(MeIn)_2L_2(OAc)]^+$ (855); $[(MeIn)_2L_2]^{2+}$ (398)
$[(MeIn)_2L_2(NO_3)(H_2O)]NO_3$ ($L = mim_3CO$)	$[(MeIn)_2L_2(NO_3)]^+$ (864); $[(MeIn)_2L_2(OAc)]^+$ (861); $[(MeIn)_2L_2]^{2+}$ (401)
$[Me_2Tl(terpy)(H_2O)]NO_3$	$[Me_2Tl(terpy)]^+$ (468)
$[Me_2Tl(phen)(H_2O)]NO_3$	$[Me_2Tl(phen)]^+$ (415); $[Me_2Tl]^+$ (235); $[phenH]^+$ (181)
$[Me_2Tl(py_2CH_2)NO_3]_2$	$[Me_2Tl(py_2CH_2)]^+$ (405); $[Tl(py_2CH_2)]^+$ (375); $[Me_2Tl]^+$ (235); Tl^+ (205)
$(Me_2Tl)_3(Et_3terpy)_2(NO_3)_3$	$[Me_2Tl(Et_3terpy)]^+$ (552); $[Tl(Et_3terpy)]^+$ (522); $[Me_2Tl]^+$ (235); Tl^+ (205)

[a] Ions observed at low ion source energies.

ion of highest m/z value observed in the ES mass spectrum at low B1 voltages is $[Me_2In(py_2CH_2)]^+$ (*m/z* 315), formed by loss of both the water and nitrato ligands. This is consistent with the labile nature of aquo indium complexes [23]. There is also a significant peak due to $[Hpy_2CH_2]^+$ (*m/z* 171), the protonated ligand, presumably formed by the same mechanism as that discussed above for $[Et_3terpyH]^+$ and a very weak peak due to $[Me_2In]^+$ (*m/z* 145). At higher B1 voltages the intensities of the *m/z* 145 and 171 peaks grow relative to that of $[Me_2In(py_2CH_2)]^+$, but no peak is observed corresponding to loss of the two methyl groups from $[Me_2In(py_2CH_2)]^+$. Data are given in Table 2.

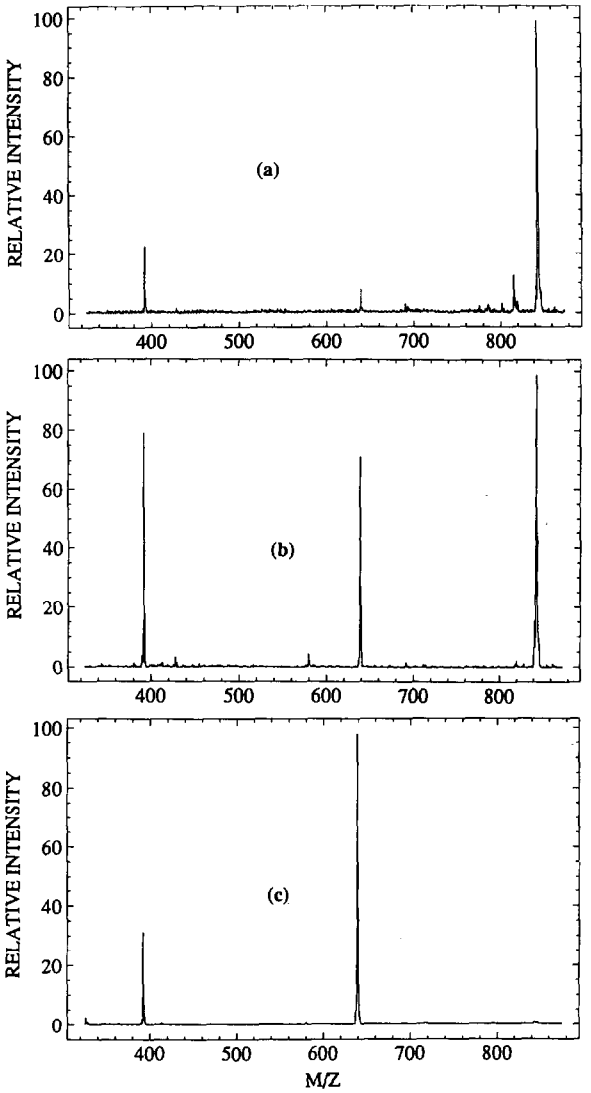

Fig. 2. Positive ion ES mass spectrum of $(MeIn)_2\{(py)_3CO\}_2(NO_3)(H_2O)]NO_3$: (a) B1 voltage = 40 V; (b) B1 voltage = 50 V; (c) B1 voltage = 80 V.

The dimeric octahedral complexes [21] whose structures are shown in Scheme 2, provide interesting ES mass spectra. At an ion source energy of 40 V, the base peak in the ES mass spectrum of $[(MeIn)_2\{(py)_3CO\}_2(NO_3)(H_2O)]NO_3$ is that due to the ion $[(MeIn)_2\{(py)_3CO\}_2(OAc)]^+$ (*m/z* 843) with a weaker peak for the ion $[(MeIn)_2\{(py)_3CO\}_2]^{2+}$ (*m/z* 392) (Fig. 2(a)) and the isotope pattern confirms the latter to be a doubly charged ion. Once again, the principal ion containing coordinated water was not observed and the coordinated nitrate is clearly readily replaced by acetate from the mobile phase to give $[(MeIn)_2\{(py)_3CO\}_2(OAc)]^+$. As the B1 voltage is increased to 60 V a peak due to a daughter ion, formed by collisions in the ion source, appears at *m/z* 639 and intensity of the peak at *m/z* 392 increases relative to that at *m/z* 843 (Fig. 2(b)). At B1 = 80 V, the peak at *m/z* 639 dominates the spectrum and no signal is observed at *m/z* 843 (Fig. 2(c)). The peak at 639 is assigned to $[In\{(py)_3CO\}_2]^+$ and its formation in the ion source confirms the labile nature of this ligand. Generally similar results were obtained for $[(MeIn)_2\{(py_2Ph)CO\}_2(NO_3)(H_2O)]NO_3$ except that in this case only $[(MeIn)_2\{(py_2Ph)CO\}_2(OAc)]^+$ (*m/z* 841) is observed at low ion source energies. However, at higher energies the ions $[(MeIn)_2\{(py_2Ph)CO\}_2]^{2+}$ (*m/z* 391) and $[In\{(py_2Ph)CO\}_2]^+$ (*m/z* 637), analogous to those described for $[(MeIn)_2\{(py)_3CO\}_2(NO_3)(H_2O)]NO_3$ are observed. The compound $[(MeIn)_2\{(pymim_2)CO\}_2(NO_3)(H_2O)]NO_3$ only gives peaks due to $[(MeIn)_2\{(pymim_2)CO\}_2(OAc)]^+$ (*m/z* 855) and $[(MeIn)_2\{(pymim_2)CO\}_2]^{2+}$ (*m/z* 398) whose relative intensities vary with B1 voltage. The compound $[(MeIn)_2\{(mim_3)CO\}_2(NO_3)(H_2O)]NO_3$ was unique in that it gave a small peak for $[(MeIn)_2\{(pymim_2)CO\}_2(NO_3)]^+$ (*m/z* 864) as well as a more intense peak for $[(MeIn)_2\{(pymim_2)CO\}_2(OAc)]^+$ (*m/z* 861). The compound also gave a weak peak at *m/z* 905, which was not identified.

2.3. Thallium(III) compounds

The dimethylthallium(III) compounds studied here also have much weaker interactions with the nitrogen bases than the gold(III) compounds. The thallium compounds for which structural information is available are shown in Scheme 3.

Even at low ion source energies (B1 = 30 V) the ES mass spectrum of the octahedral [22] complex $[Me_2Tl(terpy)(H_2O)]NO_3$ does not show the principal ion containing coordinated water, the only significant peak in the spectrum containing thallium is due to $[Me_2Tl(terpy)]^+$ (*m/z* 468) (Fig. 3(a)). This result again reflects the extreme lability of water on the group 3 metals but the terpy ligand is retained in the gas phase

despite its known lability on thallium. Figure 3(b) shows the comparison between experimental and calculated isotopic mass distributions for ion at m/z 468. The daughter ion $[Tl(terpy)]^+$ (m/z 438) appears at B1 = 60 V. MS/MS experiments show that the m/z 468 ion is stable in the gas phase. In the CAD mass spectrum the m/z 468 ion shows only three daughter ions, $[Tl(terpy)]^+$, $[terpy]^+$ and Tl^+. Very similar ES mass spectra were obtained for $[Me_2Tl(phen)(H_2O)]NO_3$ (Table 2).

In the solid state, the compound $(Me_2Tl)_3(Et_3terpy)_2(NO_3)_3$ has a structure with two $Me_2Tl(Et_3terpy)$ units bridged to a central Me_2Tl group by nitrato ligands [22] (Scheme 3). In view of the previously demonstrated lability of nitrato ligands on thallium, it was expected that the only significant peak in the mass spectrum would be that due to $[Me_2Tl(Et_3terpy)]^+$ (m/z 552) and this was found to be the case. In the CAD mass spectrum the preferred decomposition of the principal ion is by loss of the methyl groups to give $[Tl(Et_3terpy)]^+$.

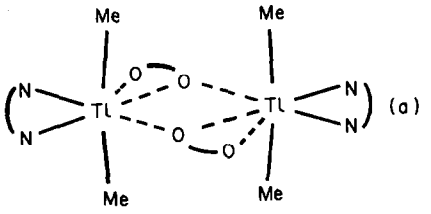

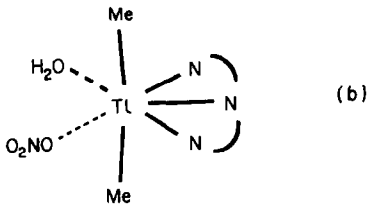

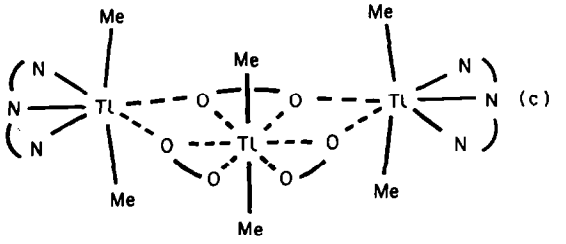

Scheme 3. Structures of Me_2Tl^{III} complexes in the solid state: (a) $[Me_2Tl(py_2CH_2)(NO_3)]^2$: TlC_2 171.7(5)°, Tl–N 2.658(9) and 2.666(9), Tl–O 2.770(9)–2.915(10) Å; (b) $[Me_2Tl(terpy)(H_2O)]NO_3$: TlC_2 169.6(6)°, Tl–N 2.620(10)–2.650(9), Tl–OH_2 2.932(12), Tl–ONO_2 3.250 (19) Å; (c) $(Me_2Tl)_3(Et_3terpy)_2(NO_3)_3$: the "aggregate" has a two-fold axis through the central thallium atom. For thallium bonded to Et_3terpy: TlC_2 166(1)°, Tl–N 2.61(3)–2.66(3); Tl–O (for entire aggregate) 2.72(2)–3.11(3) Å.

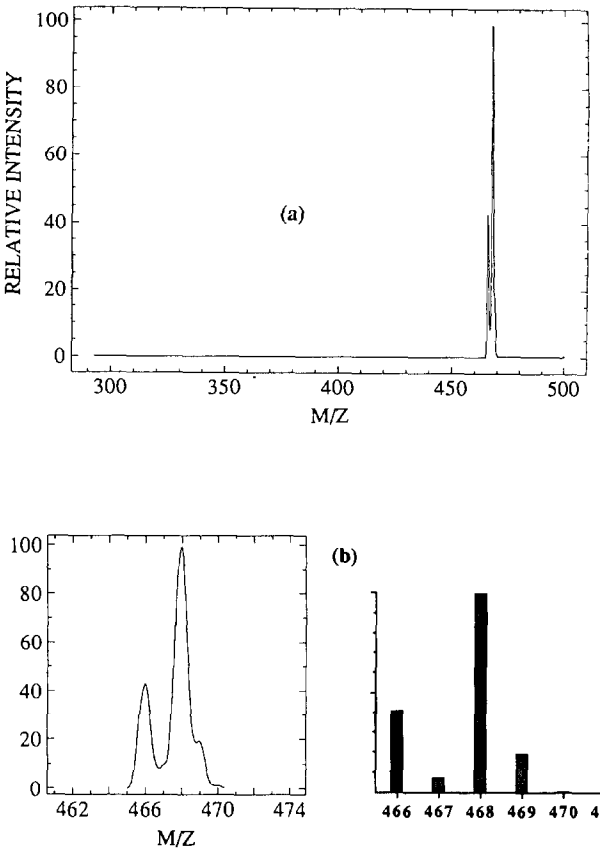

Fig. 3. (a) Positive ion ES mass spectrum of $[Me_2Tl(terpy)(H_2O)]NO_3$, B1 voltage = 30 V; (b) comparison of experimental and calculated isotopic mass distribution for the ion at m/z 468.

Although the complex $[Me_2Tl(py_2CH_2)NO_3]_2$ is dimeric in the solid state [22] with nitrato bridges, not surprisingly the ES mass spectrum at low B1 voltage shows the dominant peak to be due to $[Me_2Tl(py_2CH_2)]^+$ formed by ionisation of the nitrates. Even at B1 = 40 V there is a significant peak due to $[Me_2Tl]^+$ (m/z 235), demonstrating the extreme lability of the pyridine based nitrogen ligand, which becomes dominant at B1 = 60 V and there is only a very weak peak due to $[Tl(py_2CH_2)]^+$ (m/z 375). Even in the CAD mass spectrum of the m/z 405 ion, loss of the py_2CH_2 ligand is much the preferred pathway with only weak peaks being observed for $[Tl(py_2CH_2)]^+$ and Tl^+. These results are in marked contrast to those for the terpy derivatives, which preferentially lose methyl groups, but they are consistent with the known solution chemistry of the complexes.

3. Conclusions

One of the most important conclusions from this work is that weak interactions between the metals and ligands observed in the solid state are often retained in

the gas phase, as illustrated, for example, by the observation of $[(MeIn)_2\{mim_3CO\}_2(NO_3)]^+$ in the ES mass spectrum. However, it is known that in solution $[(MeIn)_2\{mim_3CO\}_2(NO_3)(H_2O)]^+$ is fluxional with both indium centres being equivalent on the NMR timescale in CD_3OD [21], the probable mechanism being rapid reversible dissociation of the aquo and nitrato groups and exchange with solvent. The fact that the nitrato derivative is observed in the gas phase is a reflection of the previously noted soft transfer of ions from solution to the gas phase. The variation of the relative intensities of the peaks due to $[(MeIn)_2\{mim_3CO\}_2(NO_3)]^+$ and $[(MeIn)_2\{mim_3CO\}_2]^{2+}$ as the ion source energy is varied confirms the labile nature of the nitrato group.

No ions containing coordinated water molecules or bridging nitrato groups were observed by ESMS for those species known to contain these features in the solid state. However, there is no evidence that these structures are retained in solution, particularly for those structures containing bridging nitrato ligands, and the ions actually observed are in all cases those expected to be formed by dissociation of the bridges.

4. Experimental details

Compounds were prepared as described previously [18–22].

Electrospray mass spectra were recorded by using a VG Bio-Q triple quadrupole mass spectrometer [24] with a water/methanol/acetic acid mobile phase. The compounds were dissolved in methanol (2 mM) and this solution was then diluted 1 : 10 with methanol. The diluted solution was injected directly into the spectrometer via a Rheodyne injector using a Phoenix 20 micro LC syringe pump to deliver the solution to the vaporisation nozzle of the electrospray ion source at a flow rate of 3 μl min^{-1}. Voltages at the first skimming electrode (B1) were varied between 100 V and the minimum possible consistent with retaining a stable ion jet. This varies from time to time but is usually in the range 30–35 V. Increasing the B1 voltage enhances the formation of daughter ions by collisions with solvent molecules within the ion source. In addition, ions of a particular m/z value (*e.g.* the peak maximum in an isotopic mass distribution) can be selected and passed through a collision cell into a second mass analyzer. In the absence of gas in the collision cell the stabilities of the selected ions can be investigated. Collision activated decomposition (CAD) mass spectra of the selected ions were obtained by admitting argon to the collision cell to a pressure that gave an approximately 50% reduction in the parent ion abundance, usually with an accelerating voltage of 200 V.

Acknowledgments

We thank La Trobe University for providing a SCAEF grant to assist in the purchase of the electrospray mass spectrometer.

References

1 M.R. Litzow and T.R. Spalding, *Mass Spectrometry of Inorganic and Organometallic Compounds*, Elsevier, Amsterdam, 1973.
2 J.M. Miller, *Mass Spectrom. Rev., 9* (1989) 319.
3 D.A. McCrery, D.D. Peake and M.L. Gross, *Anal. Chem., 57* (1985) 1181.
4 K.J. Kroha and K.L. Busch, *Org. Mass Spectrom., 21* (1986) 507.
5 M.I. Bruce, Cifuentes, K.R. Grundy, M.J. Liddell, M.R. Snow and E.R.T. Tiekink, *Aust. J. Chem., 41* (1988) 597.
6 G. Cetini, L. Operti, G.A. Vaglio, M. Pruzzini and P. Stoppioni, *Polyhedron, 6* (1987) 1491.
7 M. Yamashita and J.B. Fenn, *J. Phys. Chem., 88* (1984) 4451.
8 C.M. Whitehouse, M. Yamashita, J.B. Fenn and R.N. Dreyer, *Anal. Chem., 57* (1985) 675.
9 M. Yamashita and J.B. Fenn, *J. Phys. Chem., 88* (1984) 4671.
10 J.B. Fenn, M. Mann, C.K. Meng, S.F. Wong and C.M. Whitehouse, *Science, 246* (1989) 64.
11 R.D. Smith, J.A. Loo, C.G. Edmonds, C.J. Barinaga and H.R. Udseth, *Anal. Chem., 62* (1990) 882.
12 T. Braun and S. Zsindely, *Trends Anal. Chem., 11* (1992) 307.
13 R. Colton and J.C. Traeger, *Inorg. Chim. Acta, 201* (1992) 153.
14 R. Colton, J.C. Traeger and J. Harvey, *Org. Mass Spectrom., 27* (1992) 1030.
15 R. Colton, V. Tedesco and J.C. Traeger, *Inorg. Chem., 31* (1992) 3865.
16 R. Colton, B.R. James, I.D. Potter and J.C. Traeger, *Inorg. Chem.*, in press.
17 J.H. Beynon, *Org. Mass Spectrom., 12* (1977) 115.
18 A.J. Canty, N.J. Minchin, P.C. Healy and A.H. White, *J. Chem. Soc., Dalton Trans.*, (1982) 1795.
19 P.K. Byers, A.J. Canty, L.M. Engelhardt, J.M. Patrick and A.H. White, *J. Chem. Soc., Dalton Trans.*, (1985) 981.
20 P.K. Byers, A.J. Canty, N.J. Minchin, J.M. Patrick, B.W. Skelton and A.H. White, *J. Chem. Soc., Dalton Trans.*, (1985) 1183.
21 A.J. Canty, L.A. Titcombe, B.W. Skelton and A.H. White, *J. Chem. Soc., Dalton Trans.*, (1988) 35.
22 A.J. Canty, K. Mills, B.W. Skelton and A.H. White, *J. Chem. Soc., Dalton Trans.*, (1986) 939.
23 G. Wilkinson and F.A. Cotton, *Advanced Inorganic Chemistry*, 5th edn., Wiley, New York, 1988.
24 *Bio-Q*, VG BioTech, Altrincham, Cheshire, UK.